

Spectral Methods in Causal Dynamical Triangulations

Giuseppe Clemente
giuseppe.clemente@pi.infn.it



UNIVERSITÀ DI PISA

Pisa, September 23, 2019

Overview

CDT overview

phase diagram and standard results

spectral methods

spectral gap

Weyl's law and effective dimension

numerical results

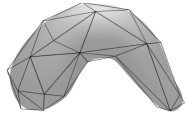
Scaling and effective dimension for slices

Critical behavior

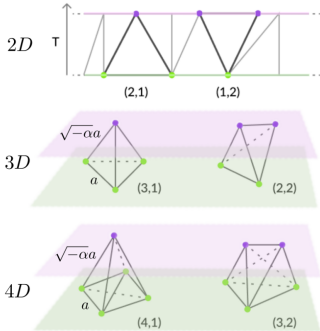
conclusions

Brief overview of CDT

Causal Dynamical Triangulations (CDT): non-perturbative Monte-Carlo approach to Quantum Gravity.



- **Simplicial manifolds** approximate smooth ones;



- A **causality condition** is enforced by considering only foliated manifolds (fixed slice topology, S^3 here);
- The action is the **Regge discretization** of the Einstein-Hilbert one;
- Wick rotation of timelike links to the Euclidean. Luckily no sign problem!
- **Continuum limit:** search for a second order critical point in the phase diagram.

Reviews: J. Ambjorn et al., Phys.Rept. 519 (2012)
R. Loll, 1905.08669 [hep-th] (2019)

Regge formalism: action discretization

Also the EH action must be discretized accordingly ($g_{\mu\nu} \rightarrow \mathcal{T}$):

$$S_{EH}[g_{\mu\nu}] = \frac{1}{16\pi G} \left[\underbrace{\int d^d x \sqrt{|g|} R}_{\text{Total curvature}} - 2\Lambda \underbrace{\int d^d x \sqrt{|g|}}_{\text{Total volume}} \right]$$

↓ discretization ↓

$$S_{\text{Regge}}[\mathcal{T}] = \frac{1}{16\pi G} \left[\sum_{\sigma^{(d-2)} \in \mathcal{T}} 2\varepsilon_{\sigma^{(d-2)}} V_{\sigma^{(d-2)}} - 2\Lambda \sum_{\sigma^{(d)} \in \mathcal{T}} V_{\sigma^{(d)}} \right],$$

where $V_{\sigma^{(k)}}$ is the k -volume of the simplex $\sigma^{(k)}$.

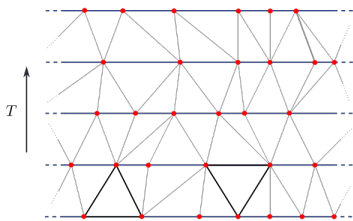
Wick-rotation $iS_{\text{Lor}}(\alpha) \rightarrow -S_{\text{Euc}}(-\alpha)$

\implies Monte-Carlo sampling $\mathcal{P}[\mathcal{T}] \equiv \frac{1}{Z} \exp(-S_{\text{Euc}}[\mathcal{T}])$

Monte-Carlo: sum over causal geometries

Configuration space in CDT: triangulations with **causal structure**

Lorentzian (causal) structure on \mathcal{T} enforced by means of a *foliation* of spatial **slices** of constant proper time.



Path-integral over causal geometries/triangulations \mathcal{T} using Monte-Carlo sampling by performing local updates. E.g., in 2D:



flipping timelike link



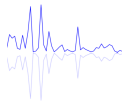
creating/removing vertex

Sketch of 4d-CDT phase diagram

k_0 and Δ parametrize the theory (related to G and Λ)

phase	spatial volume per slice
-------	--------------------------

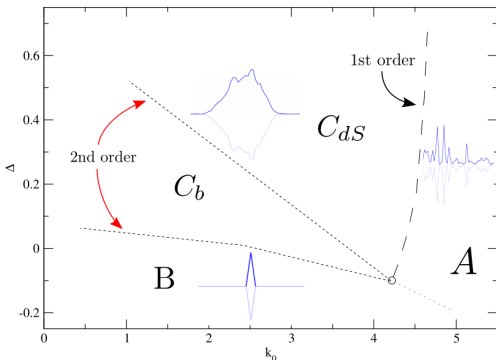
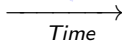
A:



B:



C_{dS}/C_b :



Possible 2nd order lines have been found.

C_{dS} spatial volume profiles compatible with *de Sitter* spacetime.

spectral methods

Spectral graph analysis of CDT slices

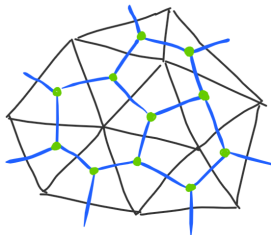
Spectral analysis

In general, the analysis of eigenvalues and eigenvector of the **Laplace-Beltrami operator**: $-\nabla^2$.

Observation

Spatial slices in CDT are made by identical $(d - 1)$ -simplexes
 \implies a d -regular undirected graph is associated to any spatial slice.

- $-\nabla^2$ becomes the Laplace matrix L of the graph dual to the sliced triangulation;
- Eigenvalue problem $L\vec{f} = \lambda\vec{f}$ solved by numerical routines.



2D slice and its dual graph

Physical interpretation of LB eigenvalues and eigenvectors

Heat/diffusion equation on a manifold (or graph) M :

$$\partial_t u(x; t) - \Delta u(x; t) = 0.$$

General solution in a basis $\{e_n\}$ of LB eigenvectors ($\lambda_n \leq \lambda_{n+1}$):

$$u(x; t) = \sum_{n=0}^{|\sigma_M|-1} e^{-\lambda_n t} \tilde{u}_n(0) e_n(x).$$

observations:

- λ_n is the diffusion rate for the (eigen)mode $e_n(x)$
- smallest eigenvalues \leftrightarrow slowest diffusion directions.
- a large **spectral gap** λ_1 implies a fast overall diffusion, geometrically meaning a highly connected graph.

Weyl's law and effective dimension

For a manifold M with LB spectrum σ_M define:

$$n(\lambda) \equiv \sum_{\bar{\lambda} \in \sigma_M} \theta(\bar{\lambda} - \lambda) = \text{“number of eigenvalues below } \lambda\text{”}.$$

Weyl's law

Well known asymptotic result from spectral geometry:

$$n(\lambda) \sim \frac{\omega_d}{(2\pi)^d} V \lambda^{d/2},$$

being ω_d the volume of a unit d -ball and V the manifold volume.

Motivated by Weyl's law we define the **effective dimension**:

$$d_{EFF}(\lambda) \equiv 2 \frac{d \log(n/V)}{d \log \lambda}.$$

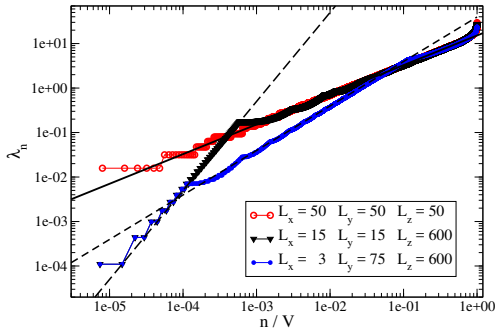
A toy model: toroidal lattice

Consider a 3-d periodic lattice with sizes $L_x \times L_y \times L_z$.

eigenvalues:

$$\lambda'_{\vec{m}} = 4\pi^2 \left(\frac{m_x^2}{L_x^2} + \frac{m_y^2}{L_y^2} + \frac{m_z^2}{L_z^2} \right),$$

with $m_i \in (-L_i/2, L_i/2] \cap \mathbb{Z}$.



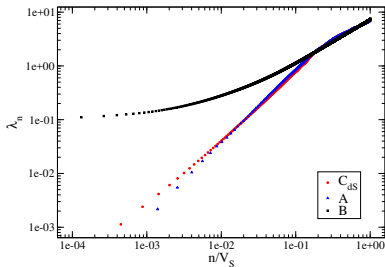
- Three regimes observed for $L_x \ll L_y \ll L_z$ with $d_{EFF} = 1, 2, 3$.
- Position of knees related to the scale of dimensional transition.

numerical results

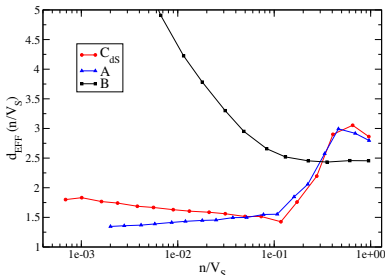
Scalings and effective dimension for different phases

G.C. and M. D'Elia [PRD 97, 124022 (2018)]

$$d_{EFF}(\lambda) \equiv 2 \frac{d \log(n/V)}{d \log \lambda}$$



Average λ in each n/V_S bin



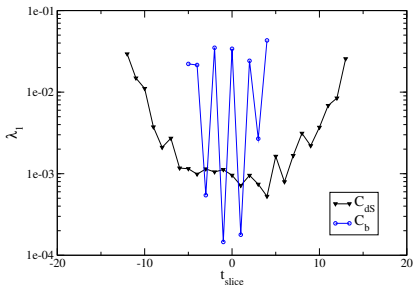
Running of effective dimension

small λ (large scale) behavior:

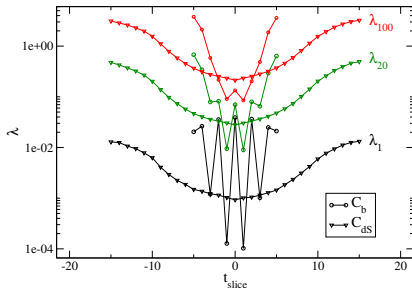
- $\lambda_1 \rightarrow 0$ and $d_{EFF} < 3$ for C_{dS} and A phases (fractional);
- $\lambda_1 \rightarrow \text{const.} > 0$ and $d_{EFF} \rightarrow \infty$ for the B phase.

The bifurcation phase C_b

Comparisons between C_{dS} and C_b low lying spectra:



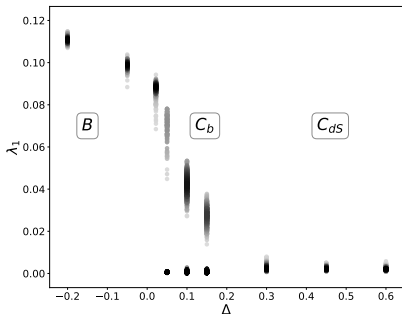
spectral gap for single configurations



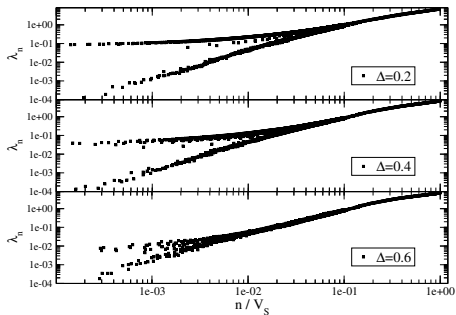
selected eigenvalues averaged over many configurations

Slices can be classified into highly connected (large λ_1) and sparsely connected (small λ_1) geometries. These classes alternate in Euclidean time.

Spectral gap in the phase diagram



Histograms of spectral gap for $k_0 = 2.2$ and different Δ .



λ_n versus n/V_S at $k_0 = 0.75$ for three values of Δ (C_b phase).

Going from C_b to C_{dS} phase **the spectral gap closes**.

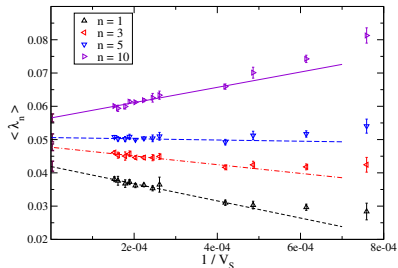
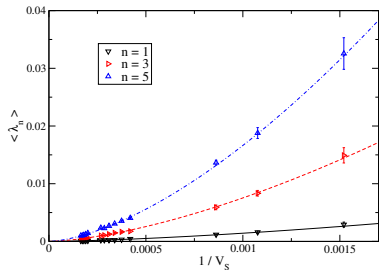
\implies we use λ_1 as an order parameter for the $C_b|C_{dS}$ transition.

Thermodynamical limits for C_b branches

- B -type and dS -type slice classes can be separately analyzed not too close the transition (class mixing).
- As for the B phase, we observe a set of distinct scales, persisting in the infinite volume limit $\langle \lambda_n \rangle_\infty$.

λ_n have dimension of a mass squared, so they seem related to a set of length scales $\xi_n \equiv \langle \lambda_n \rangle_\infty^{-1/2}$.
(i.e., the wavelength of n -th mode)

G.C., M. D'Elia and A. Ferraro [arXiv:1903.00430]

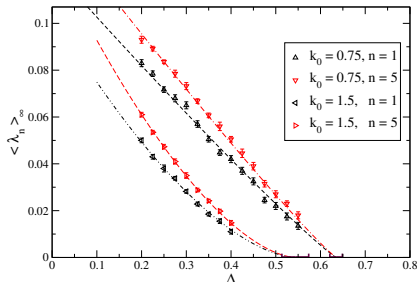


Critical behavior

Approaching the transition from the C_b phase we observe a power law behavior with **critical index** ν :

$$\langle \lambda_n \rangle_\infty = A_n (\Delta_c - \Delta)^{2\nu}. \implies \xi_n = B_n (\Delta_c - \Delta)^{-\nu}$$

- $k_0 = 0.75$ ($\chi_{\text{rid}}^2 \simeq 31/26$):
 $\Delta_c = 0.635(14)$, $\nu = 0.55(4)$.
- $k_0 = 1.5$ ($\chi_{\text{rid}}^2 \simeq 6/14$):
 $\Delta_c = 0.544(36)$, $\nu = 0.82(12)$.



All the distinct length scales ξ_n are compatible with a common critical exponent ν , as expected from a lattice field theory approaching the continuum limit.

Conclusions

Present work:

- In order to solve the lack of observables, we introduced the study of eigenvalues of the Laplace-Beltrami operator, having intuitive geometric interpretation.
- The **spectral gap** λ_1 of slices is a good order parameter for the $C_b|C_{dS}$ transition. [G.C. and M. D'Elia \[PRD 97, 124022 \(2018\)\]](#)
- We investigated further the properties of the C_b phase and the $C_b|C_{dS}$ transition: we found a hierarchy of length scales diverging with a power law, trademark of a second order phase transition. [G.C., M. D'Elia and A. Ferraro \[arXiv:1903.00430\]](#)

Work in progress:

- Analysis of the eigenvectors, containing much information worth to be investigated (e.g., mode localization).
- Spectral analysis of full space-time triangulated manifolds.
- Other projects: adding $f(R)$ terms in the action, minimal coupling with gauge theories.

additional slides

Wick rotated action in 4D

At the end of the day [Ambjörn et al., arXiv:1203.3591]:

$$S_{CDT} = -k_0 N_0 + k_4 N_4 + \Delta(N_4 + N_4^{(4,1)} - 6N_0)$$

- New parameters: (k_0, k_4, Δ) , related respectively to G , Λ and α .
- New variables: N_0 , N_4 and $N_4^{(4,1)}$, counting the total numbers of vertices, pentachorons and type-(4, 1)/(1, 4) pentachorons respectively (\mathcal{T} dependence omitted).

It is convenient to “fix” the total spacetime volume $N_4 = V$ by fine-tuning $k_4 \implies$ actually free parameters (k_0, Δ, V) .

Simulations at different volumes V allow finite-size scaling analysis.

Laplacian embedding

Laplacian embedding: embedding of graph in k -dimensional (Euclidean) space, solution to the optimization problem:

$$\min_{\vec{f}^1, \dots, \vec{f}^k} \left\{ \sum_{(v,w) \in E} \sum_{s=1}^k [f^s(v) - f^s(w)]^2 \mid \vec{f}^s \cdot \vec{f}^p = \delta_{s,p}, \vec{f}^s \cdot \vec{1} = 0 \forall s, p = 1, \dots, k \right\},$$

where for each vertex $v \in V$ the value $f^s(v)$ is its s -th coordinate in the embedding.

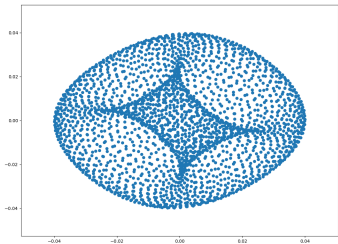
The solution $\{f^s(v)\}_{s=1}^k$ is exactly the (orthonormal) set of the first k eigenvectors of the Laplace matrix $\{e_s(v)\}_{s=1}^k$!

Laplacian embedding: example torus $T^2 = S^1 \times S^1$

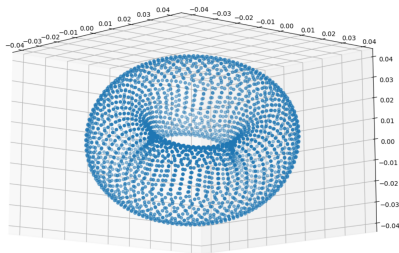
For each graph-vertex $v \in V$ plot the tuple of coordinates:

$$2\text{D: } (e_1(v), e_2(v)) \in \mathbb{R}^2$$

$$3\text{D: } (e_1(v), e_2(v), e_3(v)) \in \mathbb{R}^3$$

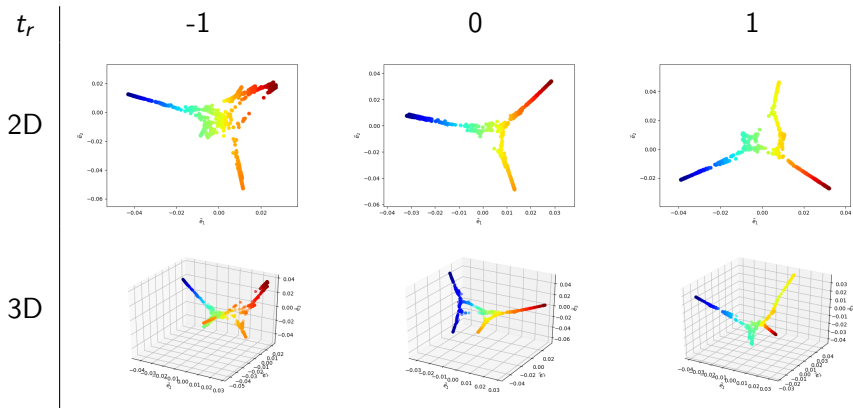


(a) 2D embedding



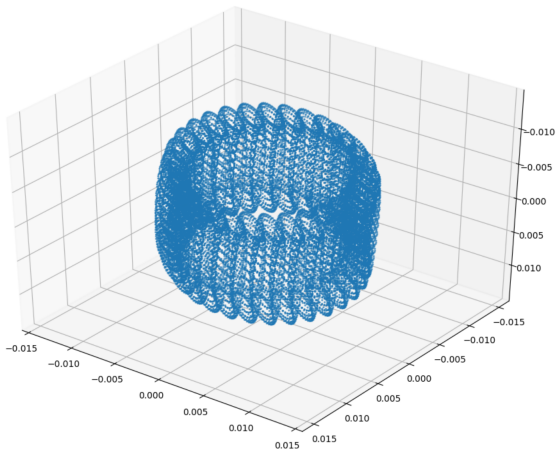
(b) 3D projected embedding

Laplacian embedding of spatial slices in C_{dS} phase



The first three eigenstates are not enough to probe the geometry of substructures

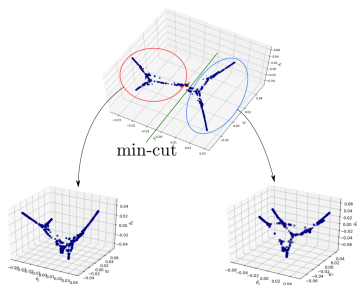
3D Laplacian embedding of T^3 torus



$$T^3 \cong T^2 \times S^1 \cong S^1 \times S^1 \times S^1$$

Result: spectral clustering of C_{dS} spatial slices

Spectral clustering: recursive application of min-cut procedure



Qualitative picture (2D)

Observation: fractality

Self-similar filamentous structures in C_{dS} phase (S^3 topology)

Spectral dimension D_S

Computed from the return probability for random-walks on manifold or graph: $P_r(\tau) \propto \tau^{-\frac{D_S}{2}} \implies D_S(\tau) \equiv -2 \frac{d \log P_r(\tau)}{d \log \tau}$.

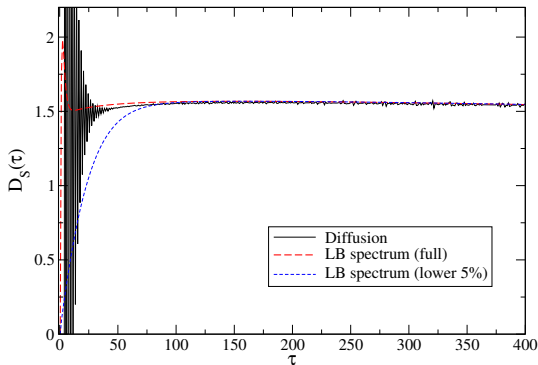
- Usual integer value on regular spaces: e.g. $D_S(\tau) = d$ on \mathbb{R}^d
- τ -independent fractional value on true fractals
- τ -dependent fractional value in general (some scale involved)

Equivalent definition of return probability: $P_r = \frac{1}{|V|} \sum_k e^{-\lambda_n t}$

\implies Nice interpretation of return probability in terms of diffusion processes (random-walks): smaller eigenvalues \leftrightarrow slower modes. The smallest non-zero eigenvalue λ_1 represents the **algebraic connectivity** of the graph.

The spectral dimension on C_{dS} slices

Compare P_r obtained by explicit diffusion processes or by the LB eigenspectrum



fractional value $D_S(\tau) \simeq 1.5 \implies$ fractal distribution of space.